Acta Cryst E CRYSTALLOGRAPHIC COMMUNICATIONS

ISSN 2056-9890

Crystal structure, Hirshfeld surface analysis and DFT study of 1-ethyl-3-phenyl-1,2-dihydroquinoxalin-2-one

Gamal Al Ati,[a] Karim Chkirate,[a] Ashraf Mashrai,[b]* Joel T. Mague,[c] Youssef Ramli,[d] Redouane Achour[a] and El Mokhtar Essassi[a]

[a]Laboratory of Heterocyclic Organic Chemistry URAC 21, Pharmacochemistry Competence Center, Av. Ibn Battouta, BP 1014, Faculty of Sciences, Mohammed V University, Rabat, Morocco, [b]Department of Pharmacy, University of Science and Technology, Ibb Branch, Ibb, Yemen, [c]Department of Chemistry, Tulane University, New Orleans, LA 70118, USA, and [d]Laboratory of Medicinal Chemistry, Drug Sciences Research Center, Faculty of Medicine and Pharmacy, Mohammed V University in Rabat, Morocco. *Correspondence e-mail: ashraf.yemen7@gmail.com

Received 3 November 2020
Accepted 2 December 2020

Edited by S. Parkin, University of Kentucky, USA

Keywords: crystal structure; dihydroquinoxaline; hydrogen bond.

CCDC reference: 2047850

Supporting information: this article has supporting information at journals.iucr.org/e

In the title molecule, $C_{16}H_{14}N_2O$, the dihydroquinoxaline moiety is not planar as there is a dihedral angle of 4.51 (5)° between the constituent rings. In the crystal, C—H···O hydrogen bonds form helical chains about the crystallographic 2_1 screw axis in the *b*-axis direction. Hirshfeld surface analysis indicates that the most important contributions to the crystal packing are from H···H (51.7%), H···C/C···H (26%) and H···O/O···H (8.5%) interactions. The optimized structure calculated using density functional theory (DFT) at the B3LYP/6–311 G(d,p) level is compared with the experimentally determined structure in the solid state. The calculated HOMO–LUMO energy gap is 3.8918 eV.

1. Chemical context

Nitrogen-based structures have attracted attention in recent years because of their interesting properties in structural and inorganic chemistry (Chkirate *et al.*, 2019; 2020*a*,*b*). The family of nitrogenous drugs, particularly those containing the quinoxaline moiety, is important in medicinal chemistry because of their wide range of pharmacological activities, which include anticancer, anti-inflammatory, antibacterial, antituberculosis, anti-glycation, anti-analgesic and antifungal properties, and for their antioxidant potential. In particular, quinoxalin-2-one derivatives are active anti-tumor agents with tyrosine kinase receptor inhibition properties (Galal *et al.*, 2014). They can also selectively antagonize the glycoprotein in cancer cells (Sun *et al.*, 2009). Quinoxalin-2-one derivatives are also potential antagonist ligands for imaging the A2A adenosine receptor by positron emission tomography (PET) (Holschbach *et al.*, 2005). Given the wide range of therapeutic applications for such compounds, we have already reported a route for the preparation of quinoxalin-2-one derivatives using *N*-alkylation reactions carried out with di-halogenated carbon chains (Benzeid *et al.*, 2011); a similar approach yielded the title compound, $C_{16}H_{14}N_2O$, (I). In addition to the synthesis, we also report the molecular and crystal structure along with a Hirshfeld surface analysis and a density functional theory (DFT) computational study carried out at the B3LYP/6–311 G(d,p) level.

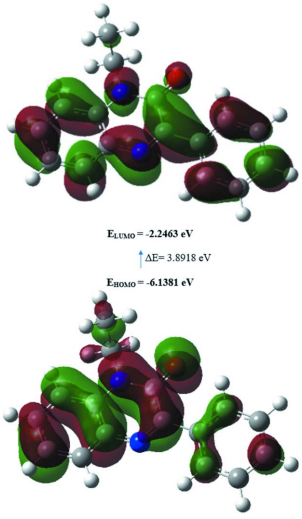

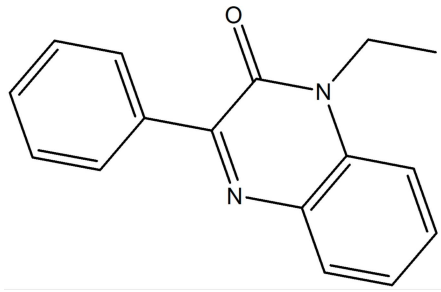

2. Structural commentary

The molecular structure of (I) is depicted in Fig. 1. The dihydroquinoxaline moiety is not planar, as indicated by the dihedral angle of 4.51 (5)° between the constituent rings. Alternatively, the maximum deviations from the mean plane (r.m.s. deviation = 0.060 Å) of the ten-membered, fused ring system are 0.096 (1) Å (C8) and −0.057 (1) Å (C7). The mean planes of the C11–C16 and C1/C6/N1/C7/C8/N2 rings are inclined to one another by 30.87 (4)°. The C6—N1—C9—C10 torsion angle is −78.78 (10)°, indicating the ethyl substituent is rotated well out of the plane of the dihydroquinoxaline moiety (Fig. 1).

3. Supramolecular features

In the crystal, helical chains about the crystallographic 2_1 axes are formed by C9—H9*B*···O1 hydrogen bonds (Table 1, Figs. 2 and 3). The chains pack *via* normal van der Waals contacts.

4. Hirshfeld surface

In order to visualize the intermolecular interactions in the crystal of the title compound, a Hirshfeld surface (HS) analysis (Hirshfeld, 1977) was carried out using *Crystal Explorer 17.5* (Turner *et al.*, 2017). A view of the three-dimensional Hirshfeld surface of (I), plotted over d_{norm} is shown in Fig. 4. The overall two-dimensional fingerprint plot (McKinnon *et al.*, 2007) is shown in Fig. 5*a*, while those delineated into H···H, H···C/C···H, H···N/N···H, H···O/O···H, C···C, C···N/N···C and C···O/O···C contacts are illustrated in Fig. 5*b*–*h*, respectively, together with their relative contributions to the Hirshfeld surface. The most important interactions are H···H, contributing 51.7% to the overall crystal packing, which is reflected in Fig. 5*b* as widely scattered points of high density due to the large hydrogen content of the

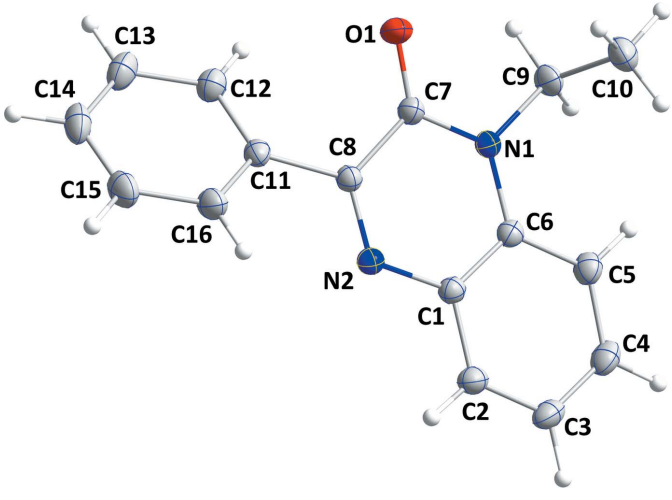

Figure 1
The title molecule with the atom-labelling scheme and 50% probability ellipsoids.

Table 1
Hydrogen-bond geometry (Å, °).

D—H···*A*	*D*—H	H···*A*	*D*···*A*	*D*—H···*A*
C9—H9*B*···O1^{i}	0.975 (13)	2.396 (13)	3.3340 (11)	161.3 (10)

Symmetry code: (i) $-x+\frac{1}{2}, y-\frac{1}{2}, -z+\frac{1}{2}$.

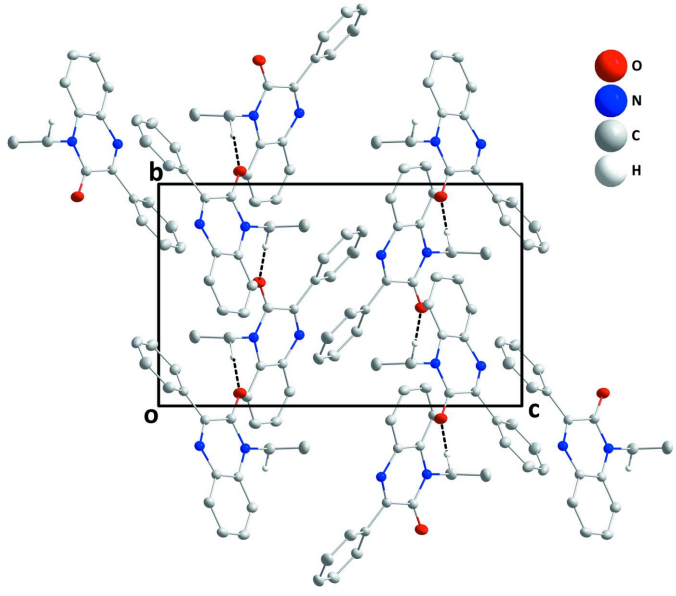

Figure 2
Packing view along the *a*-axis direction with C—H···O hydrogen bonds shown as dashed lines.

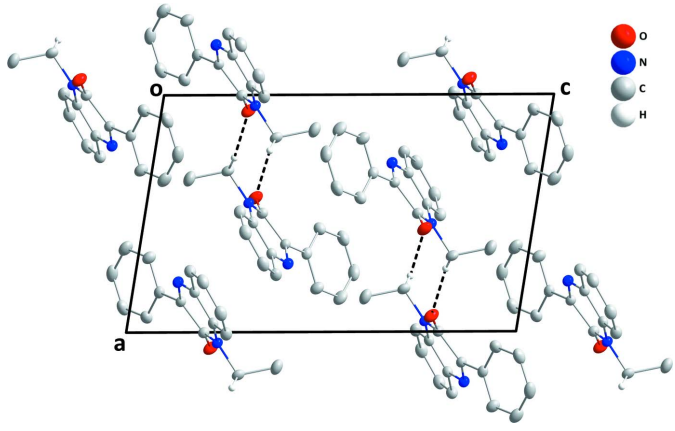

Figure 3
Packing view along the *b*-axis direction with C—H···O hydrogen bonds shown as dashed lines.

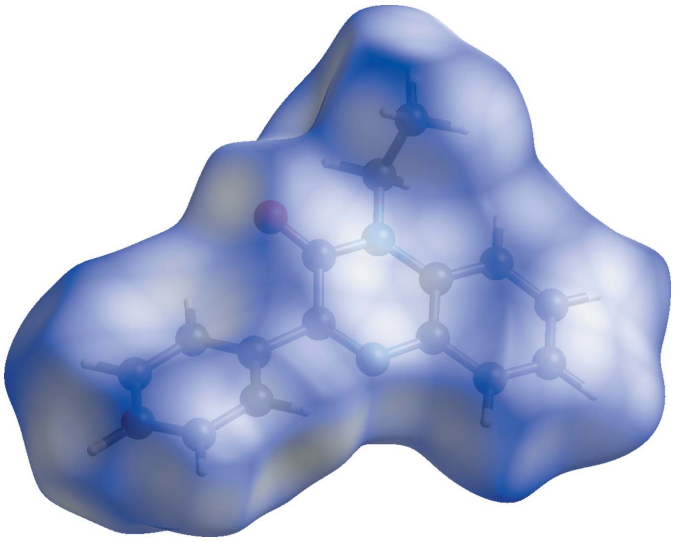

Figure 4
View of the three-dimensional Hirshfeld surface of the title compound, plotted over d_{norm}.

molecule, with the tip at $d_e = d_i = 1.07$ Å. For C—H interactions, the pair of characteristic wings in the fingerprint plot delineated into H···C/C···H contacts (26% contribution to the HS), Fig. 5*c*, have tips at $d_e + d_i = 2.79$ Å. The pair of scattered points of spikes in the fingerprint plot delineated into H···O/O···H, Fig. 5*e* (8.5%), have the tips at $d_e + d_i = 2.26$ Å. The C···C contacts, Fig. 5*f* (6.1%), have the tips at

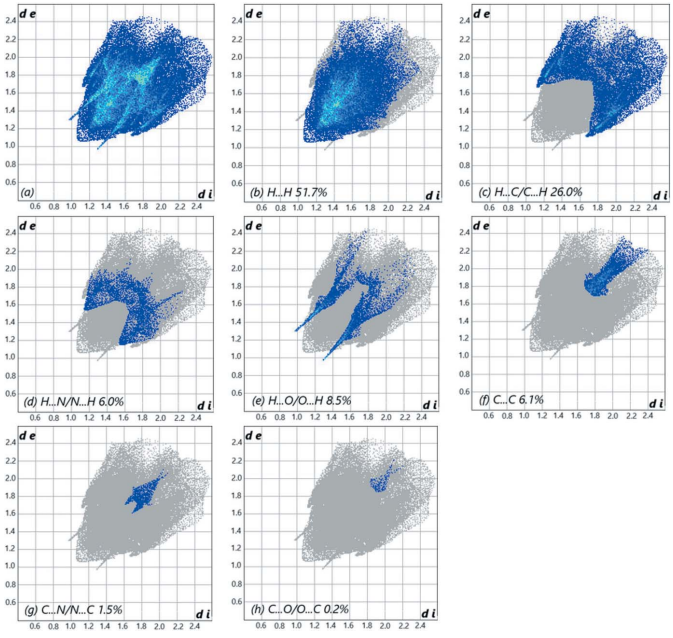

Figure 5
The full two-dimensional fingerprint plots for the title compound, showing (*a*) all interactions, and delineated into (*b*) H···H, (*c*) H···C/C···H, (*d*) H···N/N···H, (*e*) H···O/O···H, (*f*) C···C, (*g*) C···N/N···C and (*h*) C···O/O···C interactions. The d_i and d_e values are the closest internal and external distances (in Å) from points on the Hirshfeld surface.

Table 2
Comparison of selected (X-ray and DFT) bond lengths and angles (Å, °).

	X-ray	B3LYP/6–311G(d,p)
C1—C6	1.4071 (12)	1.4149
N2—C1	1.3846 (11)	1.3724
N2—C8	1.2983 (11)	1.299
C8—C11	1.4864 (11)	1.486
C7—C8	1.4872 (11)	1.4949
O1—C7	1.2299 (10)	1.2235
N1—C7	1.3791 (10)	1.3974
N1—C9	1.4732 (11)	1.4745
C9—C10	1.5156 (14)	1.5289
N1—C6	1.3936 (10)	1.3893
C6—N1—C9	120.63 (7)	121.2759
C7—N1—C6	122.16 (7)	122.6246
C7—N1—C9	117.14 (7)	116.0858
C8—N2—C1	119.29 (7)	120.9715
O1—C7—N1	121.54 (8)	120.1959
O1—C7—C8	123.36 (7)	124.593
N1—C9—C10	111.67 (7)	112.8427
N1—C6—C5	122.78 (8)	123.4659
N2—C8—C11	117.24 (7)	117.5205

Table 3
Calculated energies.

Molecular property	Compound (I)
Total energy *TE* (eV)	−21853.0851
E_{HOMO} (eV)	−6.1381
E_{LUMO} (eV)	−2.2463
Gap, ΔE (eV)	3.8918
Dipole moment, μ (Debye)	3.0212
Ionization potential, I (eV)	6.1381
Electron affinity, A	2.2463
Electronegativity, χ	4.1922
Hardness, η	1.9459
Electrophilicity, index ω	4.5158
Softness, σ	0.5139
Fraction of electrons transferred, ΔN	0.7215

$d_e + d_i = 3.45$ Å. The H···N/N···H contacts, Fig. 5*d*, contribute 6% to the HS and appear as a pair of scattered points of spikes with the tips at $d_e + d_i = 2.67$ Å. The C···N/N···C contacts, Fig. 5*g*, contribute 1.5% to the HS, appearing as pair of scattered points of spikes with the tips at $d_e + d_i = 3.30$ Å. Finally, the C···O/O···C contacts, Fig. 5*h*, make only a 0.2% contribution to the HS and have a low-density distribution of points.

5. DFT calculations

The optimized structure of (I) in the gas phase was calculated by density functional theory (DFT) using a standard B3LYP functional and the 6–311 G(d,p) basis-set (Becke, 1993) as implemented in *GAUSSIAN 09* (Frisch *et al.*, 2009). The theoretical and experimental results related to bond lengths and angles are in good agreement (Table 2). Calculated numerical values for (I) including electronegativity (χ), hardness (η), ionization potential (I), dipole moment (μ), electron affinity (A), electrophilicity (ω) and softness (σ) are collated in Table 3. The electron transition from the HOMO to the LUMO energy level is shown in Fig. 6. The HOMO and LUMO are localized in the plane extending over the whole

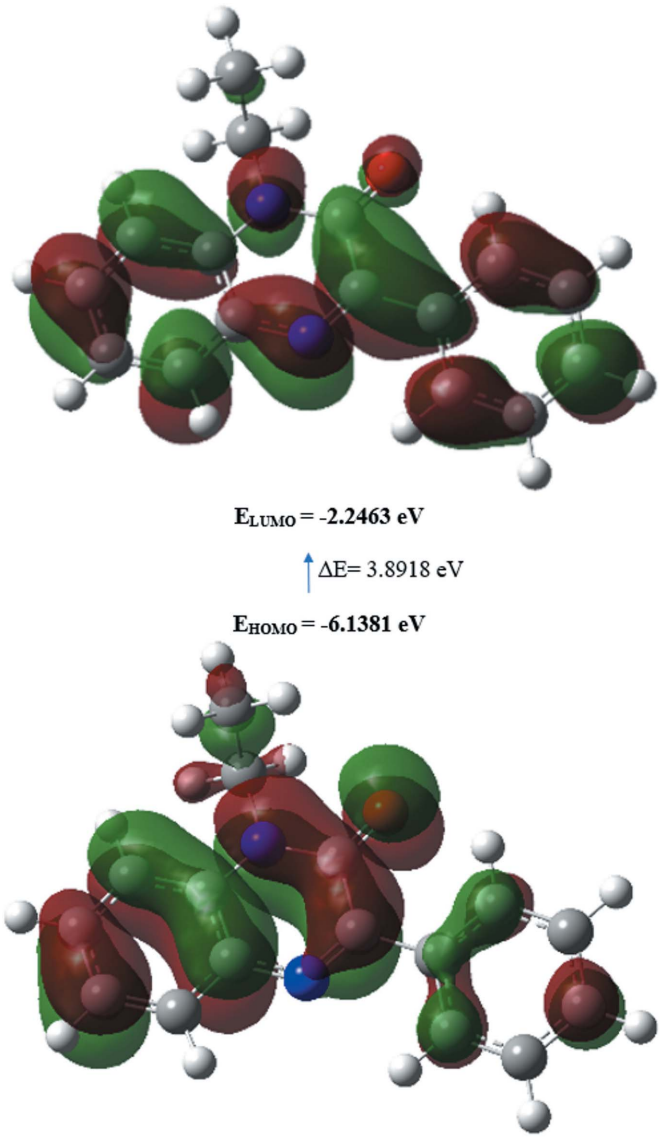

Figure 6
The energy band gap of (I).

1-ethyl-3-phenyl-1,2-dihydroquinoxalin-2-one system. The energy band gap [$\Delta E = E_{LUMO} - E_{HOMO}$] of the molecule is 3.8918 eV, and the frontier molecular orbital energies, E_{HOMO} and E_{LUMO}, are −6.1381 and −2.2463 eV, respectively.

6. Database survey

A search of the Cambridge Structural Database (CSD version 5.40, updated March 2020; Groom *et al.*, 2016) with the quinoxaline-2-one fragment yielded multiple matches. Of these, two had a phenyl at position 3 and are thus most comparable to (I). The first [(II), refcode NIBXEE; Abad *et al.*, 2018*a*)] has (oxiran-2-yl) methyl on nitrogen 1, and the second [(III), IDOSUR; Daouda *et al.*, 2013)] has a 3-ethyl-oxazolidin-2-one on nitrogen 1 (Fig. 7). Other structures having the quinoxaline-2-one moiety were observed by changing the substituents of positions 1 and 3 in the examples NAYTAJ (1-ethyl; Mamedov *et al.*, 2005*a*), DUSHUV01

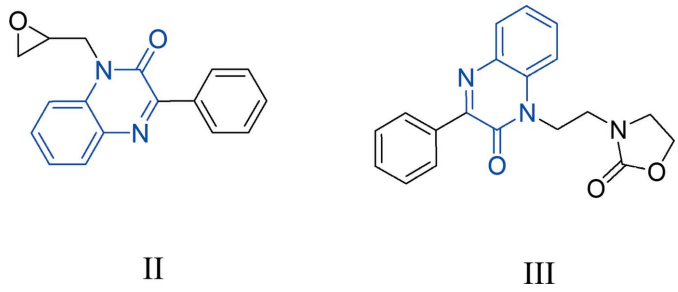

Figure 7
Structures similar to (I): (II) (CSD refcode NIBXEE) and (III) (CSD refcode IDOSUR) obtained in the database search. The search fragment is indicated in blue.

(1-benzyl-3-methyl; Ramli *et al.*, 2018), DUMRUB {1-([1-(3-azido-2-hydroxypropyl)-1*H*-1,2,3-triazol-4-yl]methyl)-3-methyl; Abad *et al.*, 2020}, HIRZOA {1- [(1-butyl-1*H*-1,2,3-triazol-4-yl)methyl]-3-methyl; Abad *et al.*, 2018*b*} and SENYUG [3- (indolizin-2-yl)-1-ethyl; Mamedov *et al.*, 2005*b*]. The dihedral angle between the dihydroquinoxaline ring system and the phenyl ring is 28.4 (2)° in NIBXEE and the N—C—C— O torsion angle is 87.8 (5)°; the mean plane through the fused-ring system forms a dihedral angle of 30.72 (5)° with the attached phenyl ring. The molecular conformation is enforced by C—H···O hydrogen bonds in IDOSUR. In (I), the dihydroquinoxaline moiety is not planar, as indicated by the dihedral angle of 4.51 (5)° between the constituent rings. The phenyl ring is tilted towards the pyrazine ring by 30.87 (4)°, which is approximately the same as in IDOSUR but more tilted than in NIBXEE.

7. Synthesis and crystallization

To a solution of 3-phenylquinoxalin-2(1*H*)-one (0.7 g, 0.0032 mol) in *N*,*N*-dimethylformamide (20 ml) were added bromoethane (0.48 ml), potassium carbonate K_2CO_3 (0.5g, 0.004 mol) and a catalytic quantity of tetra-*n*-butylammonium bromide. The reaction mixture was stirred at room temperature for 24 h. The solution was filtered and the solvent removed under reduced pressure. The residue thus obtained was separated by chromatography on a silica gel column using a hexane/ethyl acetate 9:1 mixture as eluent. The solid obtained was recrystallized from ethanol solution to afford colourless plates of the title compound (yield: 85%).

8. Refinement

Crystal data, data collection and structure refinement details are summarized in Table 4. Hydrogen atoms were included as riding contributions in idealized positions (C—H = 0.95–0.99 Å) with U_{iso}(H) = 1.2U_{eq}(C) or 1.5U_{eq}(C-methyl).

Funding information

JTM thanks Tulane University for support of the Tulane Crystallography Laboratory.

Table 4
Experimental details.

Crystal data	
Chemical formula	$C_{16}H_{14}N_2O$
M_r	250.29
Crystal system, space group	Monoclinic, $P2_1/n$
Temperature (K)	150
a, b, c (Å)	9.2572 (9), 9.0531 (9), 15.0557 (14)
β (°)	99.329 (1)
V (Å^3)	1245.1 (2)
Z	4
Radiation type	Mo $K\alpha$
μ (mm^{-1})	0.09
Crystal size (mm)	0.50 × 0.47 × 0.16
Data collection	
Diffractometer	Bruker *SMART APEX* CCD
Absorption correction	Multi-scan (*SADABS*; Krause *et al.*, 2015)
T_{min}, T_{max}	0.96, 0.99
No. of measured, independent and observed [$I > 2\sigma(I)$] reflections	23365, 3364, 2925
R_{int}	0.025
(sin $\theta/\lambda)_{max}$ (Å^{-1})	0.688
Refinement	
$R[F^2 > 2\sigma(F^2)]$, $wR(F^2)$, S	0.042, 0.130, 1.09
No. of reflections	3364
No. of parameters	228
H-atom treatment	All H-atom parameters refined
$\Delta\rho_{max}$, $\Delta\rho_{min}$ (e Å^{-3})	0.41, −0.21

Computer programs: *APEX3* and *SAINT* (Bruker, 2016), *SHELXT* (Sheldrick, 2015*a*), *SHELXL2018/1* (Sheldrick, 2015*b*), *DIAMOND* (Brandenburg & Putz, 2012) and *SHELXTL* (Sheldrick, 2008).

References

Abad, N., El Bakri, Y., Sebhaoui, J., Ramli, Y., Essassi, E. M. & Mague, J. T. (2018*a*). *IUCrData*, **3**, x180610.

Abad, N., Hajji, M., Ramli, Y., Belkhiria, M., Moftah, H., Elmgirhi, S. A., Habib, M., Guerfel, T. T., Mague, J. T. & Essassi, E. M. (2020). *J. Phys. Org. Chem.* **33**, e4055.

Abad, N., Ramli, Y., Hökelek, T., Sebbar, N. K., Mague, J. T. & Essassi, E. M. (2018*b*). *Acta Cryst.* E**74**, 1815–1820.

Becke, A. D. (1993). *J. Chem. Phys.* **98**, 5648–5652.

Benzeid, H., Bouhfid, R., Massip, S., Leger, J. M. & Essassi, E. M. (2011). *Acta Cryst.* E**67**, o2990.

Brandenburg, K. & Putz, H. (2012). *DIAMOND*, Crystal Impact GbR, Bonn, Germany.

Bruker (2016). *APEX3*, *SADABS* and *SAINT*. Bruker AXS Inc., Madison, Wisconsin, USA.

Chkirate, K., Fettach, S., El Hafi, M., Karrouchi, K., Elotmani, B., Mague, J. T., Radi, S., Faouzi, M. E. A., Adarsh, N. N., Essassi, E. M. & Garcia, Y. (2020*a*). *J. Inorg. Biochem.* **208**, 111092.

Chkirate, K., Fettach, S., Karrouchi, K., Sebbar, N. K., Essassi, E. M., Mague, J. T., Radi, S., Faouzi, M. E. A., Adarsh, N. N. & Garcia, Y. (2019). *J. Inorg. Biochem.* **191**, 21–28.

Chkirate, K., Karrouchi, K., Dege, N., Sebbar, N. K., Ejjoummany, A., Radi, S., Adarsh, N. N., Talbaoui, A., Ferbinteanu, M., Essassi, E. M. & Garcia, Y. (2020*b*). *New J. Chem.* **44**, 2210–2221.

Daouda, B., Doumbia, M. L., Essassi, E. M., Saadi, M. & El Ammari, L. (2013). *Acta Cryst.* E**69**, o662.

Frisch, M. J., Trucks, G. W., Schlegel, H. B., Scuseria, G. E., Robb, M. A., Cheeseman, J. R., Scalmani, G., Barone, V., Mennucci, B., Petersson, G. A., Nakatsuji, H., Caricato, M., Li, X., Hratchian, H. P., Izmaylov, A. F., Bloino, J., Zheng, G., Sonnenberg, J. L., Hada, M., Ehara, M., Toyota, K., Fukuda, R., Hasegawa, J., Ishida, M., Nakajima, T., Honda, Y., Kitao, O., Nakai, H., Vreven, T., Montgomery, J. A. Jr, Peralta, J. E., Ogliaro, F., Bearpark, M., Heyd, J. J., Brothers, E., Kudin, K. N., Staroverov, V. N., Kobayashi, R., Normand, J., Raghavachari, K., Rendell, A., Burant, J. C., Iyengar, S. S., Tomasi, J., Cossi, M., Rega, N., Millam, J. M., Klene, M., Knox, J. E., Cross, J. B., Bakken, V., Adamo, C., Jaramillo, J., Gomperts, R., Stratmann, R. E., Yazyev, O., Austin, A. J., Cammi, R., Pomelli, C., Ochterski, J. W., Martin, R. L., Morokuma, K., Zakrzewski, V. G., Voth, G. A., Salvador, P., Dannenberg, J. J., Dapprich, S., Daniels, A. D., Farkas, O., Foresman, J. B., Ortiz, J. V., Cioslowski, J. & Fox, D. J. (2009). *GAUSSIAN09*. Rev. A.02. Gaussian Inc., Wallingford, CT, USA.

Galal, S. A., Khairat, S. H. M., Ragab, F. A. F., Abdelsamie, A. S., Ali, M. M., Soliman, S. M., Mortier, J., Wolber, G. & El Diwani, H. I. (2014). *Eur. J. Med. Chem.* **86**, 122–132.

Groom, C. R., Bruno, I. J., Lightfoot, M. P. & Ward, S. C. (2016). *Acta Cryst.* B**72**, 171–179.

Hirshfeld, H. L. (1977). *Theor. Chim. Acta*, **44**, 129–138.

Holschbach, M. H., Bier, D., Wutz, W., Sihver, W., Schüller, M. & Olsson, R. A. (2005). *Eur. J. Med. Chem.* **40**, 421–437.

Krause, L., Herbst-Irmer, R., Sheldrick, G. M. & Stalke, D. (2015). *J. Appl. Cryst.* **48**, 3–10.

Mamedov, V. A., Kalinin, A. A., Gubaidullin, A. T., Isaikina, O. G. & Litvinov, I. A. (2005*a*). *Zh. Org. Khim.* **41**, 609–616.

Mamedov, V. A., Kalinin, A. A., Yanilkin, V. V., Gubaidullin, A. T., Latypov, Sh. K., Balandina, A. A., Isaikina, O. G., Toropchina, A. V., Nastapova, N. V., Iglamova, N. A. & Litvinov, I. A. (2005*b*). *Izv. Akad. Nauk, Ser. Khim.* **11**, 2534–2542.

McKinnon, J. J., Jayatilaka, D. & Spackman, M. A. (2007). *Chem. Commun.* pp. 3814.

Ramli, Y., El Bakri, Y., El Ghayati, L., Essassi, E. M. & Mague, J. T. (2018). *IUCrData*, **3**, x180390.

Sheldrick, G. M. (2008). *Acta Cryst.* A**64**, 112–122.

Sheldrick, G. M. (2015*a*). *Acta Cryst.* A**71**, 3–8.

Sheldrick, G. M. (2015*b*). *Acta Cryst.* C**71**, 3–8.

Sun, L.-R., Li, X., Cheng, Y.-N., Yuan, H.-Y., Chen, M.-H., Tang, W., Ward, S. G. & Qu, X.-J. (2009). *Biomed. Pharmacother.* **63**, 202–208.

Turner, M. J., McKinnon, J. J., Wolff, S. K., Grimwood, D. J., Spackman, P. R., Jayatilaka, D. & Spackman, M. A. (2017). *CrystalExplorer17. The University of Western Australia*.

supporting information

Acta Cryst. (2021). E**77**, 18-22 [https://doi.org/10.1107/S2056989020015819]

Crystal structure, Hirshfeld surface analysis and DFT study of 1-ethyl-3-phenyl-1,2-dihydroquinoxalin-2-one

Gamal Al Ati, Karim Chkirate, Ashraf Mashrai, Joel T. Mague, Youssef Ramli, Redouane Achour and El Mokhtar Essassi

Computing details

Data collection: *APEX3* (Bruker, 2016); cell refinement: *SAINT* (Bruker, 2016); data reduction: *SAINT* (Bruker, 2016); program(s) used to solve structure: *SHELXT* (Sheldrick, 2015*a*); program(s) used to refine structure: *SHELXL2018/1* (Sheldrick, 2015*b*); molecular graphics: *DIAMOND* (Brandenburg & Putz, 2012); software used to prepare material for publication: *SHELXTL* (Sheldrick, 2008).

1-Ethyl-3-phenyl-1,2-dihydroquinoxalin-2-one

Crystal data

$C_{16}H_{14}N_2O$
$M_r = 250.29$
Monoclinic, $P2_1/n$
$a = 9.2572$ (9) Å
$b = 9.0531$ (9) Å
$c = 15.0557$ (14) Å
$\beta = 99.329$ (1)°
$V = 1245.1$ (2) Å^3
$Z = 4$
$F(000) = 528$
$D_x = 1.335$ Mg m^{-3}
Mo $K\alpha$ radiation, $\lambda = 0.71073$ Å
Cell parameters from 9889 reflections
$\theta = 2.4$–29.2°
$\mu = 0.09$ mm^{-1}
$T = 150$ K
Plate, colourless
0.50 × 0.47 × 0.16 mm

Data collection

Bruker SMART APEX CCD diffractometer
Radiation source: fine-focus sealed tube
Graphite monochromator
Detector resolution: 8.3333 pixels mm^{-1}
φ and ω scans
Absorption correction: multi-scan (*SADABS*; Krause *et al.*, 2015)
$T_{min} = 0.96$, $T_{max} = 0.99$
23365 measured reflections
3364 independent reflections
2925 reflections with $I > 2\sigma(I)$
$R_{int} = 0.025$
$\theta_{max} = 29.3°$, $\theta_{min} = 2.4°$
$h = -12\rightarrow12$
$k = -12\rightarrow12$
$l = -20\rightarrow20$

Refinement

Refinement on F^2
Least-squares matrix: full
$R[F^2 > 2\sigma(F^2)] = 0.042$
$wR(F^2) = 0.130$
$S = 1.09$
3364 reflections
228 parameters
0 restraints
Primary atom site location: difference Fourier map
Secondary atom site location: difference Fourier map
Hydrogen site location: difference Fourier map
All H-atom parameters refined
$w = 1/[\sigma^2(F_o^2) + (0.0911P)^2 + 0.1012P]$ where $P = (F_o^2 + 2F_c^2)/3$

$(\Delta/\sigma)_{max} < 0.001$
$\Delta\rho_{max} = 0.41$ e Å^{-3}
$\Delta\rho_{min} = -0.21$ e Å^{-3}

Special details

Experimental. The diffraction data were obtained from 3 sets of 400 frames, each of width 0.5° in ω, collected at φ = 0.00, 90.00 and 180.00° and 2 sets of 800 frames, each of width 0.45° in φ, collected at ω = –30.00 and 210.00°. The scan time was 10 sec/frame.

Geometry. All esds (except the esd in the dihedral angle between two l.s. planes) are estimated using the full covariance matrix. The cell esds are taken into account individually in the estimation of esds in distances, angles and torsion angles; correlations between esds in cell parameters are only used when they are defined by crystal symmetry. An approximate (isotropic) treatment of cell esds is used for estimating esds involving l.s. planes.

Refinement. Refinement of F^2 against ALL reflections. The weighted R-factor wR and goodness of fit S are based on F^2, conventional R-factors R are based on F, with F set to zero for negative F^2. The threshold expression of $F^2 > 2\text{sigma}(F^2)$ is used only for calculating R-factors(gt) etc. and is not relevant to the choice of reflections for refinement. R-factors based on F^2 are statistically about twice as large as those based on F, and R- factors based on ALL data will be even larger.

Fractional atomic coordinates and isotropic or equivalent isotropic displacement parameters (Å^2)

	x	*y*	*z*	U_{iso}*/U_{eq}
O1	0.43347 (7)	0.55741 (7)	0.27640 (5)	0.02811 (19)
N1	0.45495 (8)	0.30830 (7)	0.26163 (5)	0.01831 (17)
N2	0.71192 (8)	0.31976 (7)	0.38726 (5)	0.01948 (18)
C1	0.66994 (9)	0.19050 (9)	0.34103 (6)	0.01852 (19)
C2	0.75776 (10)	0.06426 (9)	0.36083 (6)	0.0229 (2)
H2	0.8512 (14)	0.0771 (12)	0.4013 (9)	0.030 (3)*
C3	0.71308 (11)	−0.07042 (10)	0.32364 (6)	0.0254 (2)
H3	0.7731 (13)	−0.1609 (13)	0.3384 (9)	0.029 (3)*
C4	0.57963 (11)	−0.08094 (10)	0.26512 (7)	0.0262 (2)
H4	0.5463 (15)	−0.1782 (14)	0.2407 (10)	0.040 (4)*
C5	0.49306 (10)	0.04224 (10)	0.24245 (6)	0.0237 (2)
H5	0.3962 (14)	0.0325 (13)	0.2015 (9)	0.032 (3)*
C6	0.53750 (9)	0.18006 (9)	0.28052 (6)	0.01830 (19)
C7	0.49871 (9)	0.44227 (9)	0.30059 (6)	0.01918 (19)
C8	0.62953 (9)	0.43608 (9)	0.37231 (5)	0.01762 (19)
C9	0.31974 (9)	0.30696 (10)	0.19483 (6)	0.0233 (2)
H9A	0.2631 (14)	0.3931 (15)	0.2067 (9)	0.033 (3)*
H9B	0.2651 (13)	0.2186 (14)	0.2059 (8)	0.029 (3)*
C10	0.35231 (12)	0.31217 (12)	0.09942 (7)	0.0316 (2)
H10A	0.4106 (16)	0.4010 (16)	0.0903 (10)	0.043 (4)*
H10B	0.4032 (16)	0.2247 (17)	0.0845 (10)	0.047 (4)*
H10C	0.2620 (16)	0.3135 (15)	0.0563 (11)	0.048 (4)*
C11	0.66935 (9)	0.56627 (9)	0.43138 (6)	0.01939 (19)
C12	0.56472 (10)	0.66442 (10)	0.45417 (6)	0.0239 (2)
H12	0.4642 (14)	0.6541 (13)	0.4277 (9)	0.029 (3)*
C13	0.60553 (11)	0.77375 (11)	0.51836 (7)	0.0288 (2)
H13	0.5343 (14)	0.8431 (14)	0.5340 (9)	0.034 (3)*
C14	0.75007 (12)	0.78690 (11)	0.55996 (7)	0.0311 (2)
H14	0.7760 (14)	0.8637 (16)	0.6076 (10)	0.040 (3)*

C15	0.85551 (12)	0.69263 (11)	0.53570 (7)	0.0313 (2)
H15	0.9599 (15)	0.7034 (14)	0.5636 (10)	0.041 (4)*
C16	0.81542 (10)	0.58303 (10)	0.47181 (7)	0.0258 (2)
H16	0.8876 (14)	0.5150 (15)	0.4564 (8)	0.034 (3)*

Atomic displacement parameters (Å²)

	U^{11}	U^{22}	U^{33}	U^{12}	U^{13}	U^{23}
O1	0.0285 (3)	0.0206 (3)	0.0317 (4)	0.0062 (2)	−0.0059 (3)	−0.0015 (3)
N1	0.0178 (3)	0.0182 (4)	0.0182 (3)	−0.0006 (2)	0.0006 (3)	−0.0008 (2)
N2	0.0208 (3)	0.0179 (3)	0.0192 (4)	0.0000 (2)	0.0017 (3)	0.0004 (2)
C1	0.0208 (4)	0.0172 (4)	0.0180 (4)	0.0004 (3)	0.0042 (3)	0.0004 (3)
C2	0.0256 (4)	0.0208 (4)	0.0223 (4)	0.0040 (3)	0.0043 (3)	0.0021 (3)
C3	0.0346 (5)	0.0181 (4)	0.0254 (5)	0.0048 (3)	0.0103 (4)	0.0023 (3)
C4	0.0361 (5)	0.0177 (4)	0.0264 (5)	−0.0035 (3)	0.0097 (4)	−0.0020 (3)
C5	0.0279 (4)	0.0204 (4)	0.0226 (4)	−0.0041 (3)	0.0039 (3)	−0.0012 (3)
C6	0.0215 (4)	0.0169 (4)	0.0172 (4)	−0.0006 (3)	0.0051 (3)	0.0008 (3)
C7	0.0192 (4)	0.0178 (4)	0.0200 (4)	0.0001 (3)	0.0015 (3)	−0.0010 (3)
C8	0.0182 (4)	0.0172 (4)	0.0170 (4)	−0.0010 (3)	0.0014 (3)	0.0000 (3)
C9	0.0190 (4)	0.0247 (4)	0.0244 (4)	−0.0025 (3)	−0.0021 (3)	−0.0022 (3)
C10	0.0377 (5)	0.0328 (5)	0.0216 (5)	−0.0009 (4)	−0.0036 (4)	−0.0013 (4)
C11	0.0234 (4)	0.0164 (4)	0.0178 (4)	−0.0024 (3)	0.0018 (3)	0.0005 (3)
C12	0.0258 (4)	0.0226 (4)	0.0242 (4)	−0.0026 (3)	0.0066 (3)	−0.0014 (3)
C13	0.0387 (5)	0.0233 (4)	0.0271 (5)	−0.0036 (4)	0.0137 (4)	−0.0047 (4)
C14	0.0465 (6)	0.0249 (5)	0.0217 (5)	−0.0114 (4)	0.0054 (4)	−0.0050 (4)
C15	0.0337 (5)	0.0284 (5)	0.0284 (5)	−0.0075 (4)	−0.0052 (4)	−0.0023 (4)
C16	0.0251 (4)	0.0227 (4)	0.0272 (5)	−0.0014 (3)	−0.0023 (3)	−0.0015 (3)

Geometric parameters (Å, º)

O1—C7	1.2299 (10)	C9—C10	1.5156 (14)
N1—C7	1.3791 (10)	C9—H9A	0.972 (13)
N1—C6	1.3936 (10)	C9—H9B	0.975 (13)
N1—C9	1.4732 (11)	C10—H10A	0.990 (14)
N2—C8	1.2983 (11)	C10—H10B	0.966 (15)
N2—C1	1.3846 (11)	C10—H10C	0.972 (16)
C1—C2	1.4063 (11)	C11—C12	1.3976 (12)
C1—C6	1.4071 (12)	C11—C16	1.3983 (12)
C2—C3	1.3770 (13)	C12—C13	1.3920 (13)
C2—H2	0.980 (13)	C12—H12	0.955 (12)
C3—C4	1.3995 (14)	C13—C14	1.3875 (15)
C3—H3	0.995 (12)	C13—H13	0.967 (12)
C4—C5	1.3834 (13)	C14—C15	1.3893 (16)
C4—H4	0.985 (14)	C14—H14	1.000 (15)
C5—C6	1.4065 (11)	C15—C16	1.3899 (13)
C5—H5	1.006 (12)	C15—H15	0.994 (14)
C7—C8	1.4872 (11)	C16—H16	0.964 (13)
C8—C11	1.4864 (11)		

C7—N1—C6	122.16 (7)	N1—C9—H9A	107.0 (8)
C7—N1—C9	117.14 (7)	C10—C9—H9A	110.2 (8)
C6—N1—C9	120.63 (7)	N1—C9—H9B	107.3 (7)
C8—N2—C1	119.29 (7)	C10—C9—H9B	112.1 (7)
N2—C1—C2	118.35 (8)	H9A—C9—H9B	108.4 (11)
N2—C1—C6	121.76 (7)	C9—C10—H10A	110.7 (9)
C2—C1—C6	119.72 (8)	C9—C10—H10B	112.0 (9)
C3—C2—C1	120.54 (9)	H10A—C10—H10B	109.7 (12)
C3—C2—H2	122.3 (7)	C9—C10—H10C	110.6 (9)
C1—C2—H2	117.2 (7)	H10A—C10—H10C	109.0 (12)
C2—C3—C4	119.51 (8)	H10B—C10—H10C	104.7 (12)
C2—C3—H3	121.2 (7)	C12—C11—C16	118.94 (8)
C4—C3—H3	119.3 (7)	C12—C11—C8	122.45 (8)
C5—C4—C3	121.16 (8)	C16—C11—C8	118.36 (8)
C5—C4—H4	119.7 (8)	C13—C12—C11	120.11 (9)
C3—C4—H4	119.2 (8)	C13—C12—H12	119.7 (7)
C4—C5—C6	119.67 (9)	C11—C12—H12	120.1 (7)
C4—C5—H5	120.2 (7)	C14—C13—C12	120.51 (9)
C6—C5—H5	120.0 (7)	C14—C13—H13	118.7 (8)
N1—C6—C5	122.78 (8)	C12—C13—H13	120.8 (8)
N1—C6—C1	117.87 (7)	C13—C14—C15	119.73 (9)
C5—C6—C1	119.34 (7)	C13—C14—H14	119.0 (8)
O1—C7—N1	121.54 (8)	C15—C14—H14	121.2 (8)
O1—C7—C8	123.36 (7)	C14—C15—C16	120.02 (9)
N1—C7—C8	115.10 (7)	C14—C15—H15	120.3 (8)
N2—C8—C11	117.24 (7)	C16—C15—H15	119.7 (8)
N2—C8—C7	122.87 (7)	C15—C16—C11	120.64 (9)
C11—C8—C7	119.89 (7)	C15—C16—H16	120.3 (8)
N1—C9—C10	111.67 (7)	C11—C16—H16	119.0 (8)

C8—N2—C1—C2	−177.53 (8)	C1—N2—C8—C11	172.67 (7)
C8—N2—C1—C6	−2.33 (12)	C1—N2—C8—C7	−6.49 (12)
N2—C1—C2—C3	173.30 (8)	O1—C7—C8—N2	−168.24 (9)
C6—C1—C2—C3	−2.01 (13)	N1—C7—C8—N2	11.27 (12)
C1—C2—C3—C4	0.51 (14)	O1—C7—C8—C11	12.63 (13)
C2—C3—C4—C5	1.36 (14)	N1—C7—C8—C11	−167.87 (7)
C3—C4—C5—C6	−1.71 (14)	C7—N1—C9—C10	98.17 (9)
C7—N1—C6—C5	178.92 (8)	C6—N1—C9—C10	−78.78 (10)
C9—N1—C6—C5	−4.29 (13)	N2—C8—C11—C12	−148.33 (9)
C7—N1—C6—C1	−0.46 (12)	C7—C8—C11—C12	30.85 (12)
C9—N1—C6—C1	176.34 (7)	N2—C8—C11—C16	25.81 (12)
C4—C5—C6—N1	−179.18 (8)	C7—C8—C11—C16	−155.00 (8)
C4—C5—C6—C1	0.19 (13)	C16—C11—C12—C13	−2.08 (14)
N2—C1—C6—N1	5.90 (12)	C8—C11—C12—C13	172.04 (8)
C2—C1—C6—N1	−178.96 (8)	C11—C12—C13—C14	0.30 (14)
N2—C1—C6—C5	−173.50 (8)	C12—C13—C14—C15	1.64 (15)
C2—C1—C6—C5	1.64 (12)	C13—C14—C15—C16	−1.78 (15)

C6—N1—C7—O1	172.14 (8)	C14—C15—C16—C11	−0.03 (15)
C9—N1—C7—O1	−4.76 (13)	C12—C11—C16—C15	1.95 (14)
C6—N1—C7—C8	−7.37 (12)	C8—C11—C16—C15	−172.41 (9)
C9—N1—C7—C8	175.73 (7)		

Hydrogen-bond geometry (Å, º)

D—H···*A*	*D*—H	H···*A*	*D*···*A*	*D*—H···*A*
C9—H9*B*···O1^{i}	0.975 (13)	2.396 (13)	3.3340 (11)	161.3 (10)

Symmetry code: (i) −*x*+1/2, *y*−1/2, −*z*+1/2.